2020

Visual Sampling with the EEG Alpha Oscillation

Kevin Eugene Alexander
Wright State University

VISUAL SAMPLING WITH THE EEG ALPHA OSCILLATION

A thesis submitted in partial fulfillment of the
requirements for the degree of
Master of Science in Biomedical Engineering

by

KEVIN EUGENE ALEXANDER

B.S.B.E, Wright State University, 2018

2020

Wright State University

WRIGHT STATE UNIVERSITY

GRADUATE SCHOOL

July 27, 2020

I HEREBY RECOMMEND THAT THE THESIS PREPARED UNDER MY SUPERVISION BY Kevin Eugene Alexander ENTITLED Visual Sampling with the EEG Alpha Oscillation BE ACCEPTED IN PARTIAL FULFILLMENT OF THE REQUIREMENTS FOR THE DEGREE OF Master of Science in Biomedical Engineering.

_____

Sherif Elbasiouny, Ph.D.
Thesis Director

_____

John Gallagher, Ph.D.
Interim Chair, Department of Biomedical Industrial, and Human Factors Engineering

Committee on
Final Examination

_____

Sherif Elbasiouny, Ph.D.

_____

Subhashini Ganapathy, Ph.D.

_____

Assaf Harel, Ph.D.

_____

Barry Milligan, Ph.D.
Interim Dean of the Graduate School

ABSTRACT

Alexander, Kevin Eugene. M.S.B.M.E., Department of Biomedical, Industrial, and Human Factors Engineering, Wright State University, 2020. Visual Sampling with the EEG Alpha Oscillation.

The posterior alpha rhythm, seen in human electroencephalograms (EEG), is posited to originate from cycling inhibitory/excitatory states of visual relay cells in the thalamus, which could result in discrete sampling of visual information. Here, we tested this hypothesis by presenting light flashes at perceptual threshold intensity through closed eyelids to 20 participants during times of spontaneous alpha oscillations. Alpha phase and amplitude were calculated relative to each individual's retina-to-V1 conduction delay, estimated by the individuals' C1 visual-evoked potential latency. Our results show that an additional 20.96% of stimuli are observed when afferenting at V1 during an alpha wave trough (272.41°) than at peak (92.41°) phase. Additionally, the perception-phase relationship is observed at high, but not low alpha amplitudes. These results support the visual sampling hypothesis and, considering the alpha rhythm's negative correlation with attention, suggests that the alpha rhythm facilitates attention by down-sampling task-irrelevant information.

TABLE OF CONTENTS

LIST OF FIGURES

Figure Page

LIST OF TABLES

Table Page

I. INTRODUCTION

BACKGROUND

BEHAVIOR

The alpha rhythm/posterior dominant rhythm, a 7-13Hz oscillation, is a notable characteristic of the human EEG over the occipital cortex. As far back as the 1920s, the alpha rhythm has been seen to come and go with the closing and opening of the eyes, as well as during times of inactivity and task engagement (Bazanova and Vernon, 2014) and was first characterized by Hans Berger in the 1920s and 1930s (Compston, 2010). This, with the observance of similar frequencies in the auditory cortex (referred to as tau rhythm) in the absence of auditory stimuli (Tiihonen et al., 1991; Weisz et al., 2011), and sensorimotor cortex (referred to as mu rhythm) in the absence of sensorimotor engagement (Pineda, 2005; Bazanova and Vernon, 2014; Garcia-Rill et al., 2016) has led to the cortical idling hypothesis that states that 7-13 Hz is the default rhythm of cortical areas exhibited when not engaged in a task or receiving sensory input (Bazanova and Vernon, 2014).

The more modern hypothesis is that the 7-13 Hz rhythm represents sensory suppression and is largely modulated by the thalamus (Bastiaansen and Brunia, 2001; Ben-Simon et al., 2013; Omata et al., 2013; Babiloni et al., 2014). This hypothesis suggests that the alpha rhythm represents active suppression of task irrelevant cortices in order to facilitate attention (Ray and Cole, 1985; Sauseng et al., 2005; Ben-Simon et al., 2013; Babiloni et al., 2014; Limbach and Corballis, 2017; Janssens et al., 2018). It has also been found that alpha activity increases with introspective behavior (Ancoli and Green, 1977;

Yue et al., 2013) and tasks involving internally directed attention (Cooper et al., 2003; Ben-Simon et al., 2013) such as imagination (Cooper et al., 2003), mental arithmetic (Ray and Cole, 1985), autobiographical recall (Yue et al., 2013), and meditative practices (Tenke et al., 2017). This is seen as further evidence for the sensory suppression hypothesis of the alpha rhythm since internally directed attention would deem all external sensory modalities task irrelevant (Cooper et al., 2003; Ben-Simon et al., 2013). But this theory does not necessarily stand in opposition to cortical idling. Idling could easily be interpreted as inhibition of a cortical area judged to be irrelevant in the absence of incoming stimuli, this is supported by observation that alpha power decreases when sensory input is anticipated but still currently absent (Bastiaansen and Brunia, 2001; Hartmann et al., 2012; Babiloni et al., 2014; Limbach and Corballis, 2017).

Features of the alpha rhythm have also been found to have many correlates in individual personality traits. In keeping with the inhibitory function of the alpha rhythm, higher individual alpha power is positively correlated with better emotional regulation and long-term goal seeking behavior, and this is attributed to stronger thalamocortical inhibition of antisocial behaviors such as neurosis and alcoholism (Knyazev et al., 2008; Pavlenko et al., 2009). This behavioral inhibition is especially strong in individuals who show a strong decrease in alpha power in preparation of a given task (Knyazev et al., 2008) indicating better regulation of inhibition mechanisms.

As mentioned above, introspective behavior (attention directed to internal matters) has also been associated with increased alpha power. This not only reflects current task demands, but also an individual's lifestyle. For example, regardless of current beliefs or practices, it has been found that individuals who rated religion/spirituality as being an important and active part of their early life were also found to have increased posterior alpha power that persisted throughout their life (Tenke et al., 2017; Tenke et al., 2018). This is thought to be a result of meditative (introspective) practices that accompany spiritual and religious beliefs. In contrast, those who adopted spiritual or religious practices later in life were shown not to have had a subsequent increase in alpha power, suggesting that the mental habits developed early in life affect the physical development of the brain and this persists throughout the individual's lifetime (Tenke et al., 2017).

In addition to alpha power, the alpha peak frequency and band width are also found to have correlates with an individual's personality. Individuals with a higher peak alpha frequency have been found to be able process greater volumes of information at a time. And, individuals peaking at one of the extremes of the band (7 or 13 Hz) show greater originality of thought in creative tasks, whereas those nearer to 10 Hz showed decreasing originality. Similarly, an individual's alpha band width shows a strong positive correlation with their overall creativity (Bazanova and Aftanas, 2008).

FUNCTION

However, despite the long history of behavioral research and the alpha rhythm, the cellular mechanism that give rise to the oscillation and how exactly this facilitates attention is not well established. In the 1950's and 60's alpha oscillations were proposed to represent a 'neuronic shutter' (Lindsley, 1952; Callaway and Alexander, 1960) to down-sample incoming sensory information to reduce processing load, and similar discrete perceptual processes are still proposed today (VanRullen and Koch, 2003; VanRullen et al., 2014). This shutter is thought to occur at the lateral geniculate nucleus (LGN), which relays visual information to V1. At times, LGN relay cells burst- fire at 10Hz, with a hyperpolarized refractory period between bursts (Lopes da Silva, 1991; Sherman, 2001; Timofeev and Bazhenov, 2005; Timofeev and Chauvette, 2011). If many of these cells fire synchronously, visual afferentation during a widespread refractory period is less likely to be relayed to V1, resulting in a 10Hz visual shutter. Each burst in LGN relay cells results in a large excitatory postsynaptic potential (EPSP) at V1, measured as a negative deflection in the occipital EEG (Timofeev and Bazhenov, 2005), in which higher amplitudes indicating more synchronous cortical excitation (Pfurtscheller et al., 1996) that results, according to this model, from excitatory volleys from the LGN relay cells. This alpha rhythm is thought to reflect EPSPs at V1 resulting from cycling excitability in the LGN visual-relay cells, which would result in cycling visual sensitivity in phase with the alpha oscillation.

Although we do not directly test this underlying cellular mechanism here, and it should be noted that other additional mechanisms have also been proposed (as will be discussed further in the Discussion section), this thalamic mechanism has already been observed to produce alpha oscillations in animal models even with the associated phasic sampling effect on sensory transfer (Lorincz et al., 2009; Chen et al., 2016). Speculatively, sampling irrelevant information could result in a reduction in obligatory processing and hence a reduced metabolic demand such that these resources can be redirected to information deemed more task relevant. This cortical metabolic deactivation has already been shown to occur with the presence of the alpha rhythm using fMRI and NIRS techniques (Moosmann et al., 2003). Mathewson et al. (2009) refers to this sampling as the "pulsed inhibition" hypothesis and describes how a periodic decrease in sensory gain could reduce the processing load and salience (and so reducing distraction effects) of information deemed to be irrelevant. However, by not blocking out the information altogether, we are capable of being alerted to the incoming information should something potentially important occur within that sensory stream.

To more accurately measure the alpha wave phase relationship to perceptual performance, we accounted for neural conduction delays: If a visual stimulus strikes the retina at *t0*, that information arrives at the LGN at a later time, *t1*. Therefore, the excitatory state of the LGN at *t1* determines whether the visual information is relayed to V1. Further, the excitatory state of the LGN is measurable even later in the EEG, as EPSPs at V1, at *t2*. Thus, *t0* to *t2* represents the full retina-to-V1 conduction delay: At *t2*, we can assess the

excitability of the LGN at *t1*, the time of afferentation of a stimulus occurring at *t0*. This is the first study, to our knowledge, to directly examine the relationship between visual observation and spontaneous alpha phase as measured relative to each individual's conduction delay, which advances the accuracy and rigor for testing the shutter hypothesis more than before.

OBJECTIVE AND HYPOTHESIS

The objective of this study is to more robustly test the hypothesis that the alpha rhythm reflects cyclic excitability states in the visual system with a phase and timing relationship predicted by the underlying physiology and neural conduction delays. Therefore, we presented visual stimuli (at *t0*) to participants during spontaneous occipital alpha activity, then measured alpha amplitude and phase at *t2*, which was estimated by the peak latency of each individual's C1 visual-evoked potential (VEP) component (Di Russo et al., 2001). We predicted that visual stimuli at *t0* would be more likely observed with alpha phase was at a trough at *t2* (assumed to indicate an LGN excitatory state at *t1*) than at a peak (an inhibitory state at *t1*). Additionally, this alpha phase effect was predicted to be greater at high alpha amplitudes, indicating greater synchrony in the underlying cellular excitatory state.

To make these measurements, we binned the trials by alpha amplitude at *t2* into high and low amplitude bins (based on median split), and then binned once more by alpha phase at *t2* into 90° wide bins centered at 0°, 90° (peak), 180°, and 270° (trough). The percentage of trials reported as being observed within each bin was then calculated, and this was

termed the binned observation rate (OR). And so, amplitude and phase were the experiment's independent variables, and OR was the dependent variable. Our predictions were specifically that OR would be greatest in the 90° phase condition, and least in 270° phase condition, but that this phase effect on OR would be most pronounced in the high amplitude condition than in the low amplitude condition.

Our results show that the OR was 20.96% greater at alpha phase trough that at alpha phase peak at *t2* when alpha amplitude was high. At low amplitude, no significant effect of phase on OR was observed. These results support our hypothesis that the alpha rhythm reflects cyclic excitatory states in the visual system resulting in a visual shutter effect. These results could help to explain the well-established negative correlation between the alpha rhythm and attention.

II. MATERIALS & METHODS

PARTICIPANTS

Alpha activity varies largely both within (Gonçalves et al., 2006) and between (Wieneke et al., 1980) individuals. For this study, we needed to ensure stimuli were able to be presented during times of observable (e.g., stationary) alpha oscillations and therefore selected participants who more readily and reliably generated observable occipital alpha activity. This selection was made by observing EEG activity as the participants practiced the visual sensitivity task with eyes closed during an earlier portion of the experimental session. Participants who did not readily and reliably produce occipital alpha oscillations during this practice period were excluded from further participation.

In total, 41 participants were recruited for this study. Based on the observable alpha criteria described above, 21 participants were excluded from further participation. The remaining 20 healthy participants (10 males/10 females, mean age: 22.3 years, range: 18-28 years) completed two tasks: one to estimate their individual conduction delay; the other to investigate their visual sensitivity at different phases of alpha oscillations. The experimental protocol was approved by the Institutional Review Boards of Wright State University and the Air Force Research Laboratory. All participants were compensated for their time.

RECORDING

All recordings were made using the BioSemi ActiveTwo system (BioSemi B.V., Amsterdam, The Netherlands). Recordings were made with a 2048 Hz sampling rate at 64

channel locations based on the modified combinatorial nomenclature extension of the 10-10 system (American Electroencephalographic Society, 1994) excluding the inferior chain with the exception of P9/P10 and Iz (Seeck et al., 2017), with bilateral electrodes on the mastoid process, infraorbital, and outer canthus locations. Participant responses were recorded using a low-latency mechanical keyboard (Cherry MX 6.0 [G80-3930], Cherry GmbH, Auerbach in der Oberpfalz, Germany). This was combined with other task-state and visual-stimulus timing information via light sensors placed on the monitor to record events on the ActiveTwo's 16-bit trigger line (StimTracker 1G, Cedrus Corporation, San Pedro, California, USA).

STIMULI

All tasks and stimuli were constructed and presented using MATLAB (R2011b; The MathWorks, Inc., Natick, MA, USA) and the Psychophysics Toolbox (v3.0.13) (Brainard, 1997; Pelli, 1997; Kleiner et al., 2007). This software was run on a Dell Precision T3610 computer (Dell Inc., Round Tock, TX, USA) with the Windows 7 Professional operating system (Microsoft Corporation, Redmond, WA, USA). Stimuli were presented to participants on a 24.5", 240 Hz monitor (BenQ ZOWIE XL2540, BenQ Corporation, Taipei, Taiwan) providing 4.2 ms temporal resolution for stimulus presentation. Where relevant, stimulus luminance was measured using a light meter (Light Meter LUX/FC 840020, SPER SCIENTIFIC, Scottsdale, AZ, USA). The participant's head position was fixed using a chinrest placed 58 cm from this monitor. The experiment was conducted in a

dark room with a natural sound machine (Dohm Classic, Marpac LLC, Wilmington, NC, USA) to mask noise disturbances.

DATA ANALYSIS

All data analyses were performed in MATLAB (R2019b; The MathWorks, Inc., Natick, MA, USA) utilizing the EEGLAB Toolbox (v2019.0) (Delorme and Makeig, 2004) and the ERPLAB plugin (v7.0.0) (Lopez-Calderon and Luck, 2014). Statistical analyses were conducted using MATLAB's Statistics and Machine Learning Toolbox (R2019b; The MathWorks, Inc., Natick, MA, USA). This software was run on a Lenovo ThinkPad P50 computer (Lenovo, Morrisville, NC, USA) with the Windows 10 Enterprise operating system (Microsoft Corporation, Redmond, WA, USA).

ESTIMATION OF *T2*

The peak latency of each participant's C1 visual-evoked potential (VEP) component was used as an estimate of their individual retina-to-V1 conduction delay, *t2*. This component reflects the arrival of visual information to the primary visual cortex from the LGN along the optic radiations. However, due to the specific folding of the V1 cortical area around the calcarine fissure (Figure 1A), the C1 wave shape will vary with the location of the stimulus in the visual field. Stimuli presented horizontally centered in the visual field will stimulate spatially opposing V1 neurons whose dipoles will cancel each other out, yielding no measurable C1 component in the EEG (Clark et al., 1995; Di Russo et al., 2001). This is similarly the case for stimuli presented approximately 3° below the vertical

center (Clark et al., 1995; Di Russo et al., 2001). However, with some horizontal spacing, bilateral stimuli presented above -3° in the visual field will produce a negative C1 wave, while those presented below -3° in the visual field will produce a positive C1 wave as shown in Figure 1B (Clark et al., 1995; Di Russo et al., 2001).

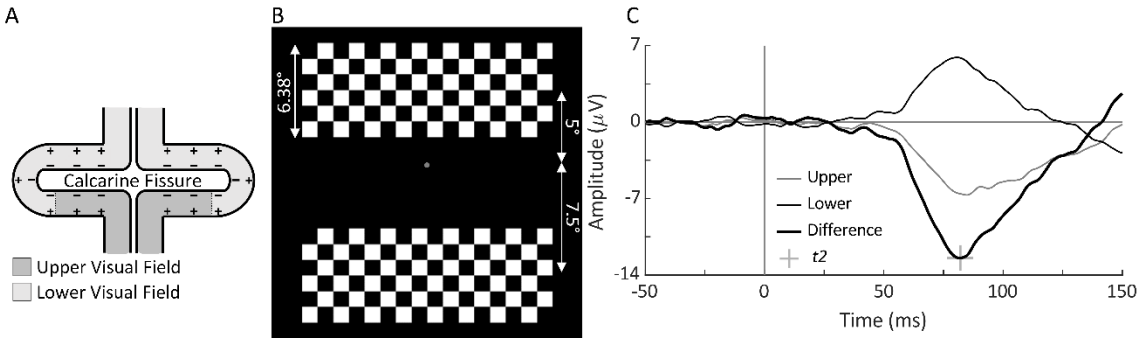

Figure 1. Methods of estimating *t2*. (A) According to the cruciform model of the calcarine fissure in the V1 cortical area, the lower portion of the fissure will respond to upper visual field stimuli and vice versa for the upper portion of the fissure. For this reason, and as the upper and lower portions of the fissure contain opposing dipoles, upper and lower visual field stimuli will create waveforms of opposing polarity in the EEG. (B) Upper and lower visual field stimuli used for C1 VEP task are centered 3° below the fixation point to account for the overrepresentation of the lower visual field in the calcarine fissure as shown in (A). (C) C1 VEP from a single participant in response to the upper and lower stimuli, the difference was measured as the lower minus the upper VEP. The peak latency of the difference wave (indicated as '+') was used as the estimate of *t2*

C1 waves are found to be measured maximally at electrode POz using an averaged mastoid reference, but they are still quite small in amplitude. To obtain a well-defined C1 VEP component, both negative and positive components were obtained using upper and lower visual field stimuli. Next, the difference between these two signals was taken to create a large-amplitude wave with a clear peak (Figure 1C shows these waveforms from a single participant). This peak latency was taken as an estimate of *t2*.

EXPERIMENTAL DESIGN

The stimulus used for this task was a 17° wide, 6.38° tall black and white checkerboard made of 16x6 1.06° squares placed on an otherwise black screen with a fixation point placed in the center (Figure 1B). The checkerboard was flashed with its center either 5° above or 7.5° below the fixation point and centered horizontally. The size and placement of these stimuli were selected to generate maximum amplitude waves (Clark et al., 1995). A total of 600 upper and 600 lower stimuli were presented in a mixed random order each with a duration of 33 ms with random 250-450 ms interstimulus-intervals, resulting in a trial time of approximately 7.5 minutes.

Similarly to Di Russo et al. (2001), participant attention and gaze were maintained on the fixation point by a sham task performed during the trial. The fixation point would occasionally flash to a brighter color for 12.6 ms, and the participant was instructed to watch for this flash and to respond by pressing the space bar.

ANALYSIS

For the C1 VEP analysis, the originally recorded 2048 Hz sampling rate was maintained but re-referenced to averaged mastoids. All EEG signals were band-pass filtered from 0.01 to 50 Hz at -6 dB, using a 2nd order IIR Butterworth filter as implemented in the ERPLAB toolbox (Lopez-Calderon and Luck, 2014), to achieve a zero-phase filter response. A bipolar vertical electrooculogram (vEOG) signal was created by subtracting the averaged left and right infraorbital electrodes from the averaged Fp1 and Fp2 electrodes.

The data were epoched from 50 ms prior to 200 ms after stimulus presentation for both the upper and lower visual stimuli. Blinks within these epochs were detected by sliding a 150 ms window at 75 ms steps over the vEOG signal, and any window containing a peak-to-peak amplitude of 100 μV or greater was rejected from analysis. Separate average VEPs were calculated for the upper and lower stimulus trials and were baseline-corrected to the 50 ms pre-stimulus period. The lower visual field VEP was then subtracted from the upper field VEP to create a difference wave containing a C1 wave with a clear peak.

The C1 peak latency was measured at electrode POz by finding the most negative peak within the 0-110 ms time window relative to stimulus onset. This peak latency was calculated for each participant individually and was used as an estimate of their individual *t2*.

MEASURING OBSERVATION RATES

This task was designed to be conducted with closed eyes in order to evoke more frequent (Legewie et al., 1969) and higher amplitude alpha oscillations (Barry et al., 2007). For this purpose, stimuli were designed such that they could be observed as light flashes through closed eyelids. The brightness of these flashes was designed to be near threshold intensity (where participants reported seeing approximately 50% of the stimuli) to prevent any ceiling or floor effects on performance.

EXPERIMENTAL DESIGN

The stimulus used for this task was an 8.5° square centered on an otherwise black (0.7 lux) screen. The stimulus brightness was defined by coloring the square as a greyscale value from 0 (completely black; 0.7 lux) to 255 (completely white; 89.2 lux). The stimulus was designed to be observable through the closed eyes of the participants. The brightness of the stimulus was adjusted to near the threshold intensity for each individual participant, the value at which each participant reported observing the stimulus half of the number of times it was presented. This threshold was estimated using the staircase method as described in Cornsweet (1962) during a calibration task prior to the main task. In this task, the participant kept their eyes closed as a series of flashes were presented, each time the participant reported observing a flash (using the spacebar) the stimulus intensity was decreased in the next trial. However, if the participant did not report observing the stimulus, the intensity was increased on the next trial. Following the methods described in Cornsweet (1962), threshold intensity is defined as the average of all trials following the third reversal in trial-intensity slope. An example of this task from one participant is shown in Figure 2. In this figure, the third reversal occurred at trial 5, and threshold intensity was calculated as the average of trials 6 to 40.

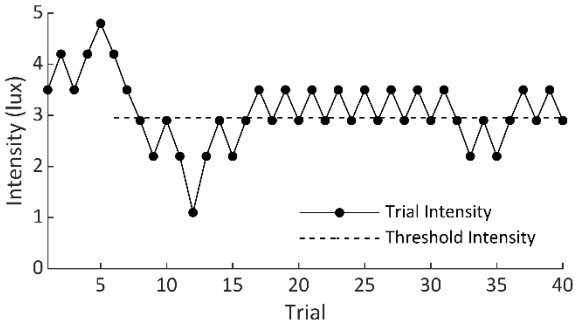

Figure 2. Example of the staircase method used to determine the threshold intensity in a single participant. Each time the participant observed the stimulus, the intensity in the next trial was decreased. If the participant did not observe the stimulus in one trial, the intensity was increased in the next trial. Threshold intensity was determined as the average intensity of all trials (trials 6-40 in this example) following the third reversal, or corner, in the trial-intensity trace (trial 5 in this example). The dashed threshold intensity line in this figure spans the trials over which the intensities were averaged.

The stimuli used were so dim that the participants' ability to perceive them was sensitive to how well their eyes had adapted to the dark. Pilot testing of the task revealed that, without an adjustment period, the threshold brightness found during the calibration task would become easier to see over the course of the main task. Although visual adaptation to the dark will continue over many hours, the most rapid changes occur in the first 15 minutes, and visual acuity begins to plateau in 20 minutes (Bierings et al., 2018). Therefore, participants were given 25 minutes in the dark as an adaptation period before conducting the calibration task to estimate the threshold brightness.

In the main task, the stimuli were flashed for a period of 8.4 ms and the participants were instructed to respond using the keyboard spacebar any time they observed, or thought they observed, a flash. The participant had to respond within two seconds of the stimulus presentation to be considered as a valid response.

It was the goal to have as many trials presented during times of well-developed alpha oscillations as possible. To accomplish this, the experimenter controlled when the stimuli were presented, manually triggering the onset whenever this rhythm was observed in the real-time data stream throughout the task. A single experimenter conducted every experiment in order to maintain some consistency in this judgment. Also, to mitigate any potential confounding effects of experimenter bias in stimulus prestation timing, a random interval of less than 750 ms was added between the trigger and the actual presentation of the stimulus. Admittedly, a better method to accomplish this would be to measure posterior alpha power in real time and to have the stimulus presentation automated based on some threshold power; this would remove any experimenter bias. However, due to limitations on equipment and time, this on-line analysis was not accomplished for the present experiment.

ANALYSIS

All data were down-sampled to 512 Hz and re-referenced to averaged mastoids. The signal was bandpass filtered from 0.01 to 50 Hz at -6dB using a 2nd order IIR Butterworth filter, as implemented in the ERPLAB toolbox (Lopez-Calderon and Luck, 2014), to achieve a zero-phase filter response. A bipolar vEOG signal was created by subtracting the averaged left and right infraorbital electrodes from the averaged Fp1 and Fp2 electrodes.

To isolate the activities of the left and right visual cortices, a left occipital (LO) signal was calculated by averaging the channels O1, PO3, and PO7, and a right occipital (RO) signal was calculated by averaging channels O2, PO4, and PO8. LO and RO were then convolved with a 10 Hz complex Morlet wavelet to obtain time-domain power and phase

signals (Cohen, 2014). A peak-to-peak amplitude signal was then calculated by doubling the square root of the power signal.

The Morlet wavelet was constructed with a center frequency of 10 Hz containing 22/3 cycles (the recommended minimum (Cohen, 2019)). This cycle count was chosen to optimize temporal resolution and resulted in a wavelet with a full-width at half maximum (FWHM) of 101.6 ms in the time domain and 8.87 Hz in the frequency domain. A FWHM of 8.87 Hz indicates that the wavelet convolution was effectively a bandpass filter with half-power points of 5.57 and 14.44 Hz, approximating the alpha frequency band.

The following analysis was then performed independently for each participant. Amplitude and phase were measured from LO and RO at the individuals' *t2* relative to stimulus onset for both observed and missed trials. Trials in which LO and RO phases differed by more than 90° were rejected from further analysis to control for alpha asynchrony between the hemispheres. For each of the remaining trials, a single amplitude and phase value was obtained by averaging the amplitude and phase of the LO and RO signals. Phase values were averaged using appropriate statistics for circular quantities (Berens, 2009). These trials were then divided by median amplitude into high and low amplitude bins and then further divided by phase using 90° bins centered on 0°, 90°, 180°, and 270° phase angles. Condition specific observation rates (OR, the percentage of trials in which the participant observed the stimulus) were then calculated for every bin resulting in an OR value for each of the 2 (amplitude) x 4 (phase) bins.

STATISTICAL ANALYSIS

This analysis resulted in a within-subjects 2x4 repeated measures design with twenty participants and two factors: amplitude (high, low) and phase (0°, 90°, 180°, 270°). These data were analyzed using a repeated measures ANOVA, testing both main effect of amplitude and phase as well as their interaction. Independent t-test and Tukey's HSD tests were used to probe any effects found to be significant. All statistical analyses were conducted using MATLAB's Statistics and Machine Learning Toolbox (R2019b; The MathWorks, Inc., Natick, MA, USA).

III. RESULTS

INDIVIDUAL RETINA-TO-V1 CONDUCTION DELAY (*T2*) MEASUREMENT

In the first part of the experiment, the goal was to estimate each participant's retina-to-V1 conduction delay, *t2*. To calculate that, we measured in each participant the averaged VEPs in response to upper and lower visual stimuli and calculated the "difference waveform" (based on the difference between two signals); the peak latency of this difference waveform was taken as the participant's *t2* (Figure 3). The mean *t2* for all participants was 75.56 ms (range = [62.99, 88.87] ms, 95% confidence interval (CI) = [72.44, 78.69] ms). These data indicate that it takes, on average, 75.56 ms for visual information to be transmitted from the retina to area V1. For each participant, the phase and amplitude measurements were made at the individual's *t2* relative to the stimulus onset to assess visual sensitivity.

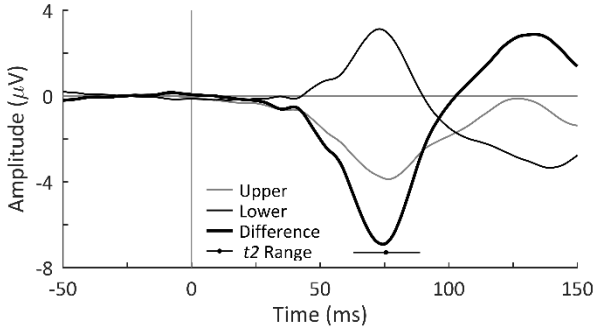

Figure 3. C1 VEP component averaged across all participants in response to upper and lower visual field stimuli. The Difference waveform is the Lower waveform subtracted from the Upper waveform. The mean and range of each participant's estimated retina-to-V1 conduction delay (*t2*) is indicated and was calculated as the peak latency of the C1 component in each individual's Difference waveform

OBSERVATION RATE MEASUREMENT

The second part of the experiment aimed to investigate if perceptual performance, when measured at *t2*, is higher at an alpha wave trough (i.e., phase angle of 270°) than an alpha wave peak (i.e., phase angle of 90°). To examine this, we presented light flashes to each participant through closed eyes. Light flashes were near individual threshold intensity estimated using the staircase method (Cornsweet, 1962) during a calibration task prior to the main task to prevent ceiling and floor performance effects. This resulted in the stimuli of average luminance across participants of 6.48 lux. Use of these near-threshold stimuli resulting in total observation rates averaging 58.28% across participants.

In total, participants were presented 161.65 stimuli on average during the main task (range = [120, 200]) where variability in trial count was due to the frequency of alpha burst occurrence during the experimental period. Interstimulus intervals averaged 12.52 seconds. Left occipital (LO) and right occipital (RO) amplitude and phase signals were measured for each participant and analyzed at the participant's *t2* time point, trials in which LO and RO phases differed by more than 90° were rejected from further analysis resulting in 135.75 trials remaining per participant on average (range = [85, 183]) . The amplitude measures were split by their median value into two bins (high and low), and the phase measures were split into four 90° bins centered on 0°, 90°, 180°, and 270° phase angles. These phase bins in order contained on average across participants 16.15, 15, 14.05, and 16.95 trials in the high amplitude condition, and 18.15, 18.5, 17.75, and 19.2 trials in the low amplitude condition. This indicates that trial counts in each of the eight conditions

were roughly balanced. A within-subjects 2 (amplitude) x 4 (phase) repeated measures ANOVA analysis was conducted on the participant OR values. Mauchly tests indicated no significant violation in the assumption of sphericity for phase ($\chi2(5) = 10.169$, $p = 0.0706$), or the interaction of phase and amplitude ($\chi2(5) = 3.250$, $p = 0.6615$). The ANOVA analysis showed that phase and the interaction between phase and amplitude have statistically significant effects on observation rates, as shown in Table 1. Accordingly, these ANOVA results support our hypothesis that a relationship between alpha phase and visual observation exists, and that this relationship is modulated by the alpha wave amplitude.

Table 1. At *t2,* two (amplitude) x four (phase) within-subjects repeated measures ANOVA results.

Source	Statistic	*p*	η_p^2	Power
phase	F(3,57) = 7.971	0.0002	0.2955	0.986
amplitude	F(1,19) = 1.751	0.2014	0.0844	0.242
phase*amplitude	F(3,57) = 3.770	0.0154	0.1656	0.786

Multiple comparison tests were performed to investigate the precise nature of the effects found to be significant in the ANOVA. Figure 4 shows the results of independent t-tests (significance indicated by #) comparing the OR of each bin to the overall OR. Only phase bins 90° and 270° in the high amplitude condition were found to be significantly different [$t(19) = -5.632$, $p = 0.0002$; $t(19) = 3.466$, $p = 0.0207$ respectively, Bonferroni corrected for eight comparisons (Bland and Altman, 1995)]. Tukey's HSD tests (indicated by *) then compared the OR distributions between phase bins within each amplitude level.

These tests found significant differences in the phase bins only in the high amplitude condition. Specifically, the 90° phase bin was statistically different from the 0° ($p = 0.0077$), 180° ($p = 0.0308$), and 270° ($p < 0.0001$) phase bins in the high amplitude condition (Figure 4). Importantly, the greatest difference in the high amplitude condition was found between phase bins 90° and 270°, with a 22.20% increase in observation rates (95% CI = [9.77% , 34.63%], Figure 4). Collectively, these results show that stimuli are observed with greatest probability when the alpha wave is near a trough at *t2*, and with lowest probably when near a peak, when alpha amplitude is high. The perception-phase relationship is robust only at high alpha wave amplitude, likely because during low amplitude oscillations the measured phase is less representative of the underlying neural population activity.

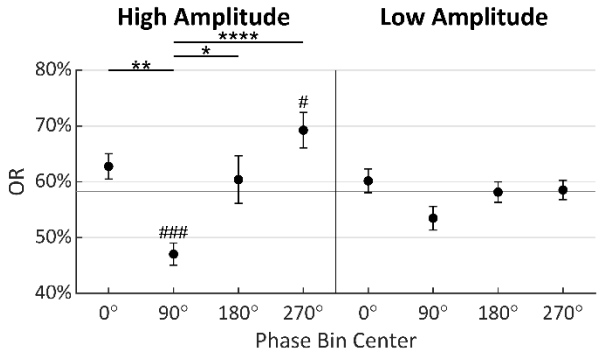

Figure 4. At *t2*, observation rate (OR) for each amplitude and phase condition.Condition specific OR relative to overall OR (marked by dark horizontal line) with bars indicating standard errors. Tukey's HSD tests were performed between phase levels within amplitude conditions with significance indicated by '*'. Bonferroni corrected t-tests compared each condition specific OR to the overall OR with significance indicated by '#'. 90° = peak. ([*,#]: p≤0.05, [**,##]: p≤0.01, [***,###]: p≤0.001, [****,####]: p≤0.0001).

PHASE-VARYING ANALYSIS OF VISUAL OBSERVATION

For a better view of the phase effect, we repeated the original procedure at *t2* using 90° phase bins rotated in 1° increments for all 360° phase angles, in order to obtain a smooth ΔOR distribution. Figure 5 shows this OR for each of the twenty participants in both the high and low amplitude conditions as a function of the centered alpha phase angle of the bins. Indicated along the circumference is the direction of the center of mass of these phase diagrams for each condition, calculated as the angle of the vector mean of each of the 360 points forming the OR distribution. This angle is referred to here as the preferred phase and indicates the phase at which stimuli have the highest probability of being observed given the whole distribution. Note that in the high amplitude condition, the preferred phase is between 180° and 360° (the negative portion of the alpha cycle) in eighteen out of the twenty participants. These preferred phase angles have associated magnitudes indicating how far the distribution's center of mass is offset in that direction and the strength of the effect of phase on observation rates. These preferred phase angles and magnitudes for all participants are shown in Figure 6, panels B and D.

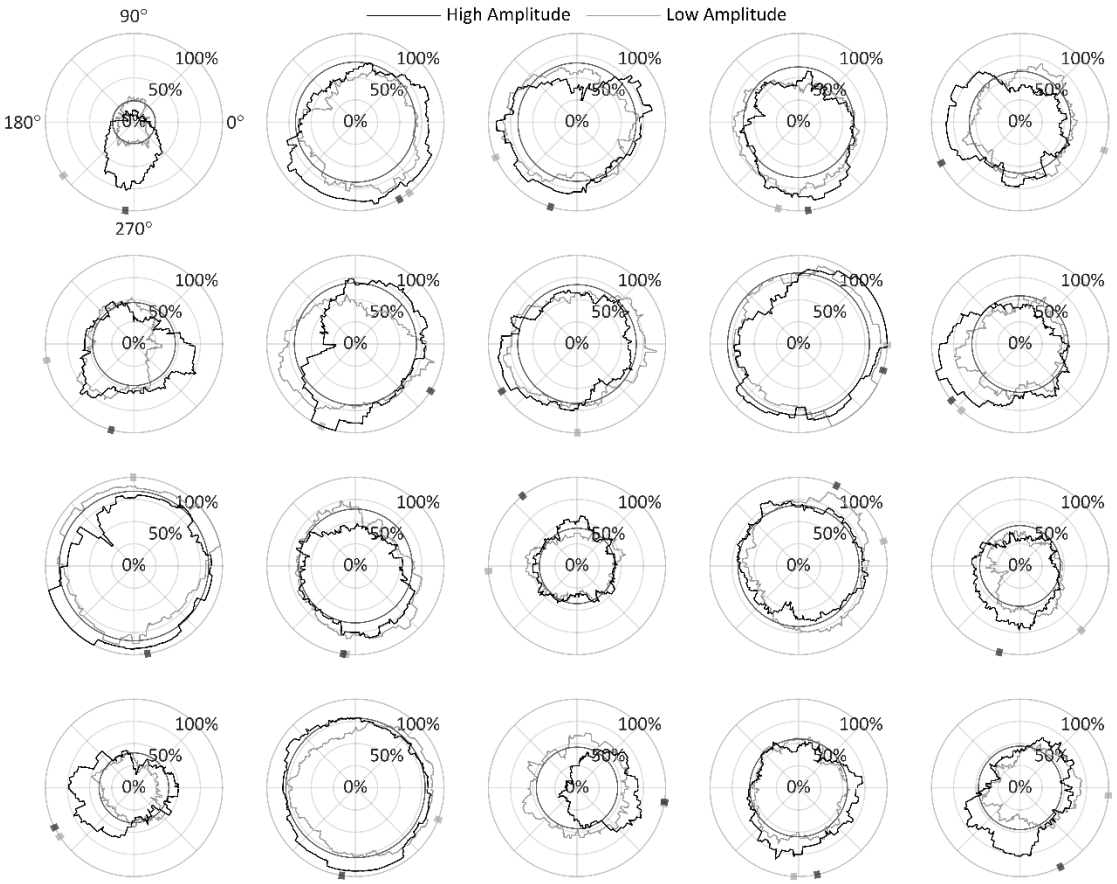

Figure 5. At *t2*, OR as a function of phase for each participant.Each value represents the observation rate in the high and low amplitude condition relative to the overall observation rate (indicated by the darkened circle). The preferred phase is indicated on the circumference, calculated as the direction towards the circle's center of mass. 90° = peak.

Figure 6, panels A and C, show the OR distributions averaged across all participants. Indicated in black along the circumference is the group's preferred phase. Note that calculating the group's preferred phase as the direction to the center of mass of the group's OR distributions (Figure 6, panels A and C) is equivalent to calculating the vector mean of

the twenty individual preferred phases and associated magnitudes (Figure 6, panels B and D). By taking the OR value at the preferred phase angle and subtracting from it the corresponding opposite phase angle (by 180°, referred to as the pessimal phase), we obtain what will be referred to here as the preferred phase effect (PPE), which indicates the increase in OR from pessimal to preferred alpha phase angles, relative to *t2*. Our results showed that the preferred phase was similar in both the high and low amplitude conditions (272.41° and 284.65°, respectively) with a PPE of 20.96% in the high amplitude condition but 9.12% in the low amplitude condition. These data further substantiate an interaction effect on observation probability between alpha wave phase and amplitude, which was observed in the prior ANOVA analysis.

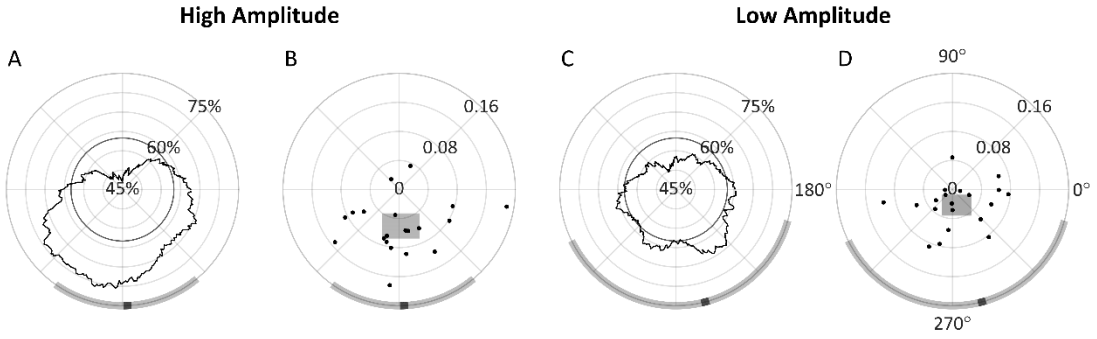

Figure 6. At *t2*, OR as a function of phase for all participants.Panels A and C show OR as a function of phase, with radial axis extending to negative values. The darkened circle represents the overall OR. Panels B and D show individual participants' preferred phase angles; their magnitude is proportional their individual preferred phase effect. The width and height of the shaded rectangles indicate, respectively, the X and Y 95% CI in cartesian space. In all panels, the group mean preferred phase is indicated in black on the circumference of the diagrams, with the shaded region indicating estimated 95% CIs for each amplitude condition. 90° = peak.

Additionally, 95% confidence intervals (CI) were estimated for the group's preferred phase and are indicated as the shaded regions along the circumference of the phase diagrams. These CIs could only be estimated since there is not a known method of computing an angular CI on non-unit vectors directly. To estimate these CIs, the twenty individual preferred phase vectors (with associated magnitudes) were first converted to cartesian values. Then, two 95% CIs were calculated separately on both the X and Y components, indicated respectively as the width and height of the shaded rectangles in Figure 6, panels B and D. The angular interval that encompassed both CIs was then used to represent the estimated 95% CI on the preferred phase in the polar space, although this interval will not necessarily be centered on the preferred phase (i.e., mean). In the high amplitude condition, this resulted in an estimated 95% CI of [234.75°, 309.84°], and in the low amplitude condition a much wider CI of [206.22°, 344.45°]. Together with Figure 6A and B, these results show that observations rates are highest at the trough of the alpha wave, and lowest at the peak. This effect is prominent in the high amplitude condition, but also to a much lesser extent in the low amplitude condition recalling these effects did not reach significance in the prior ANOVA.

MEASURING INDUCED ACTIVITY

Alpha band desynchronization and phase resetting are characteristically observed in response to relevant visual stimuli (Klimesch et al., 2011). It is important to ensure that the amplitude and phase measurements made here are the result of spontaneous brain activity and not simply induced by the stimulus itself. The percent change in alpha amplitude,

relative to a prestimulus baseline period of -300 to -100 ms, was first calculated for both the observed and missed trials and is shown in Figure 7. As would be expected, there is very little change in alpha amplitude in response to missed stimuli. However, there can be seen the characteristic drop in amplitude in response to observed stimuli. But this drop in amplitude is not induced until sometime later than 100 ms post stimulus indicating the measurements made at *t2* were safe from stimulus induced amplitude effects.

Phase coherence across all trials, as well as just the observed and missed trials, was also calculated and shown in Figure 7 to ensure there was no event related phase resetting, which would be measured as an increase in phase coherence after stimulus onset. As seen in Figure 7, no phase resetting is apparent in the observed trials or in all trials together until after 150 ms where a small upward trend can be seen. No event related phase resetting would be expected in the missed trials, and of course this is not seen. But, in the phase coherence across missed trials, there is a prominent peak measured at the 70.31 ms time point. This should not be interpreted as an event related phase reset, however, since it is the peak of an upward trend starting at least 300 ms prior to stimulus onset, this will be discussed further in the Discussion section. Also, note the overall increase in phase coherence values of the observed and missed trials compared to that of all trials combined. This is expected since, according to the phase effects on observation rates found above, trials that are observed and missed will predominantly occupy specific, opposing phase ranges. This would result in relatively high phase coherence across trials when grouped by observational outcome, and low when grouped together. Overall, Figure 7 shows that there

is no event related amplitude change or phase reset prior to 100 ms post stimulus indicating that the phase and amplitude measures taken for this study are not the result of stimulus induced activity, but of ongoing spontaneous oscillations.

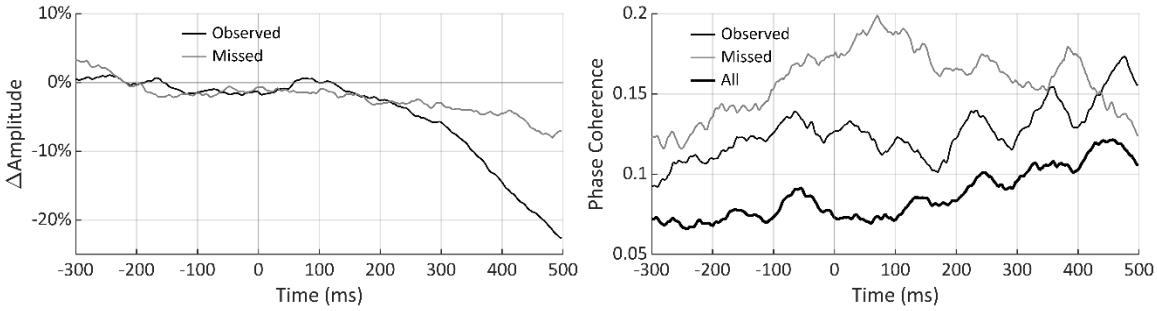

Figure 7. Measures of induced oscillatory activity.Change in alpha amplitude, relative to a -300 to -100 ms baseline interval, and alpha phase coherence for observed and missed stimuli, and all stimuli together in the phase coherence panel. These figures show no indication of stimulus induced oscillatory effects at the t2 time point where phase and amplitude measures were made.

T2 MEASUREMENTS IMPROVE ON PRESTIMULUS MEASUREMENTS

To evaluate the benefit of the using the individual *t2* time point at which to measure the alpha phase effect on perceptual performance, the above analysis was repeated instead at a time point 100 ms prior to stimulus onset. These types of measurements are more frequently made in prestimulus periods or at stimulus onset in order to avoid measuring induced oscillatory effects as mentioned above. Whereas in the previous analysis, the four phase bins centered at 0°, 90°, 180°, and 270° were chosen a priori based on their theoretical significance at the *t2* time point, no prediction could be made about the relevant phase bins at this prestimulus time point. Instead, the analysis was first performed in 90° phase bins in 1° increments, as was performed previously (i.e. Figure 6), and the four

relevant phase bins were chosen empirically based on the preferred phase in the high amplitude condition.

The results of this analysis performed over 360 90° bins in both the high and low amplitude conditions are shown in Figure 8. In the high amplitude condition, a phase effect on perceptual performance can again be observed, however in this case the preferred phase was measured at 33.53° (95% CI = [-354.87°, 40.33°]) with a 15.48% PPE. In the low amplitude condition, the preferred phase was measured at 342.78° (95% CI = [326.04°, 19.99°]) with a 5.22% PPE.

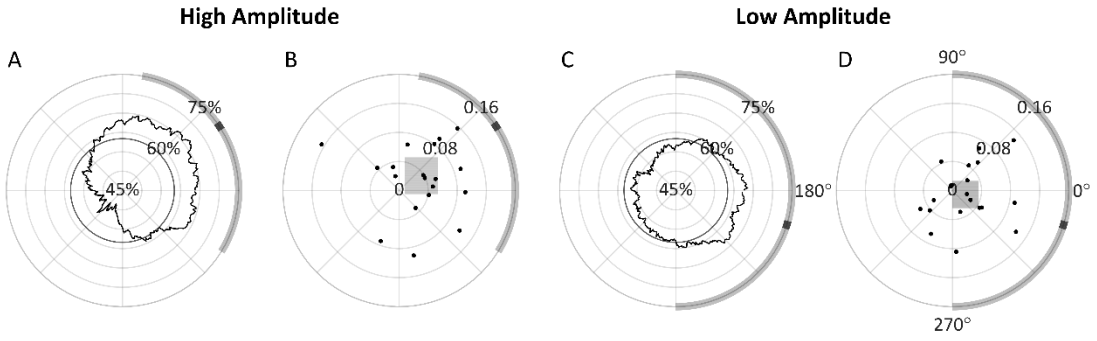

Figure 8. At t = -100ms, OR as a function of phase for all participants.Panels A and C show OR as a function of phase, with radial axis extending to negative values, the darkened circle represents the overall OR. Panels B and D show individual participants' preferred phase angles. The width and height of the shaded rectangles indicate, respectively, the X and Y 95% CI in cartesian space. In all panels, the group mean preferred phase is indicated in black on the circumference of the diagrams, with the shaded region indicating estimated 95% CIs for each amplitude condition. 90° = peak.

Based on the preferred phase measured in the high amplitude condition, the four 90° phase bins centered at 33°, 123°, 213°, and 303° were chosen for the 2x4 repeated measures ANOVA analysis. Mauchly tests indicated no significant violation in the assumption of

sphericity for phase ($\chi2(5) = 5.194$, $p = 0.3926$), or the interaction of phase and amplitude ($\chi2(5) = 8.861$, $p = 0.1147$). As shown in Table 2, only the main effect of phase was found to have a statistically significant effect on observation rates, however in this case the effect size is nearly half of what was found when conducting this same analysis at *t2*.

Table 2. At t = -100ms, two (amplitude) x four (phase) within-subjects repeated measures ANOVA results.

Source	Statistic	*p*	η_p^2	Power
phase	F(3,57) = 3.378	0.0243	0.1510	0.735
amplitude	F(1,19) = 0.008	0.9289	0.0004	0.051
phase*amplitude	F(3,57) = 1.695	0.1784	0.0819	0.420

Figure 9 shows the multiple comparisons result for this data collected at 100 ms prior to stimulus onset for better comparison to those from *t2* shown in Figure 4. Bonferroni corrected independent t-tests compared each condition specific OR value to the overall OR, but none were found to be significant, indicating that none of the OR values in any of these four phase bins differed from the overall mean observation rate either amplitude condition. Tukey's HSD tests (indicated by *) were used to compare OR distributions between phase bis within each amplitude level, but these tests only found a significant difference between 33° and 213° ($p = 0.0143$) where there was a 15.47% difference in observations rates (95% CI = [2.39%, 28.55%]). These results show that although an alpha phase effect on

observation rates in a prestimulus period can be observed, the strength of the effect is much weaker than when measurements are taken at *t2*.

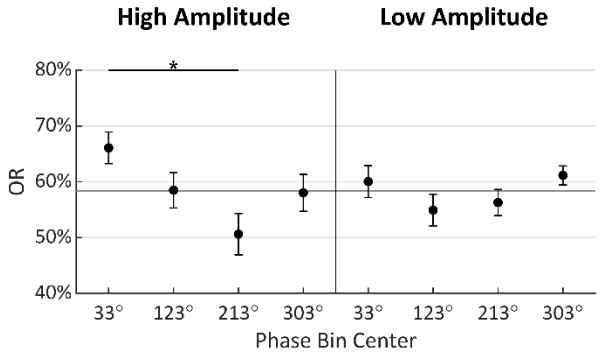

Figure 9. At t = -100ms, observation rate (OR) for each amplitude and phase condition.Condition specific OR relative to overall OR (marked by dark horizontal line) with bars indicating standard errors. Tukey's HSD tests were performed between phase levels within amplitude conditions with significance indicated by '*'. Bonferroni corrected did not find any of the condition specific OR to significantly differ from the overall OR. 90° = peak. (*: $p \leq 0.05$).

IV. DISCUSSION

This study presents a novel, controlled method for examining the neuronic shutter effect, hypothesized to be reflected in the posterior alpha oscillations observed in human EEG. Our hypothesis was that perceptual performance fluctuates with the alpha rhythm in a precise phase and timing relationship. To test this relationship, we (1) presented near-threshold intensity visual stimuli through closed eyes to participants; (2) accounted for individual retina-to-V1 conduction delays (*t2*); (3) controlled for asynchrony between hemispheres; and (4) measured the alpha phase and amplitude relative to *t2*. Our results confirm a robust relationship between the alpha rhythm phase and perception, with the greatest rates of observation occurring at the alpha wave trough (excitatory state) and the lowest rates at the alpha wave peak (inhibitory state). The perception-phase relationship appears to be modulated by alpha amplitude as it is observed at high, but not low, alpha wave amplitude. This work is novel in considering the underlying neural structure and function of the visual system when predicting the exact phase relationship to perception, and in controlling for individual neural conduction delay and asynchrony between hemispheres.

While the alpha wave shutter effect has been previously examined (Dustman and Beck, 1965; Mathewson et al., 2009; Mathewson et al., 2012; Milton and Pleydell-Pearce, 2016; Kizuk and Mathewson, 2017), this is the first study, to our knowledge, to directly examine the relationship between perceptual performance and spontaneous alpha phase as measured relative to each individual's conduction delay. Previous studies have either

measured alpha phase at stimulus onset, *t0*, or during prestimulus periods (Mathewson et al., 2009; Mathewson et al., 2012; Milton and Pleydell-Pearce, 2016; Kizuk and Mathewson, 2017). Accordingly, the phase measurements were not always well aligned with the LGN excitability state according to the proposed cellular mechanism. Here, when we accounted for each individual's conduction delay, as opposed to the group average conduction delay or measuring at stimulus onset *t0*, we demonstrated a robust relationship between the alpha phase and perception. Notably, these results provide the most robust evidence consistent with cyclic LGN excitability as the cellular mechanism mediating this effect – though we do not directly examine this mechanism. One study (Dustman and Beck, 1965) measured reactions times, as opposed to observation rates, at alpha phase adjusted to group average, as opposed to individual conduction delay. This study, similar to ours, found slowest reaction times at the peak (90°) of the alpha wave, and fastest reaction times close to the alpha trough (240°).

A 2x4 repeated measures ANOVA found that alpha phase at *t2* had a significant effect on perceptual performance as hypothesized. The interaction effect of phase and amplitude was also found to be significant; the multiple comparisons tests in Figure 4 show that low amplitude attenuates the phase effect. This supports the hypothesis that low amplitude alpha waves reflect asynchronous inhibition within the visual system. Although not part of our original hypothesis, it is somewhat surprising that no main effect of amplitude was found since alpha power has sometimes been found to predict perceptual performance (Ergenoglu et al., 2004; Mathewson et al., 2009; Bruers and VanRullen, 2018). Figure 6

gives a higher phase angle resolution view of the effects seen in Figure 4. In both the high and low amplitude conditions, the preferred phase was near the wave trough (272.41° and 284.65° at high and low amplitude, respectively). However, in the low amplitude condition, the 95% CI of the preferred phase was much wider, and the PPE was lower (20.96% and 9.12% at high and low amplitude, respectively). These results show how alpha amplitude modulates the effect of alpha phase on perception.

It appears that the most defined effect of the alpha oscillation is its inhibitory phase. This is reflected by the Tukey's test in the high amplitude condition shown in Figure 4, as well as the measured phase coherence shown in Figure 7. The Tukey's test found that observations rates at the zero crossing phases (0° and 180°) were significantly higher than that of the peak phase, but not significantly lower than the observation rates measured at the trough phase. Similarly, phase coherence was greater across missed trials than observed trials. These two findings indicate that stimuli are most likely to be missed just at the peak phase, but more likely to be observed at any other phase including the zero crossings or trough. It is also important to note that the missed trial phase coherence trace features a prominent peak at 70.41 ms. This peak should not be interpreted as an event related phase reset since 1) it is the peak of an upward trend beginning at least 300 ms prior to stimulus onset, 2) a decreasing trend is observed immediately afterwards, and 3) no phase reset would be expected in response to an unobserved stimulus. Instead, this peak is probably best interpreted as marking the time where phase most accurately predicts that a stimulus will not be observed. The gradually decreasing phase coherence values before and after

this peak likely represent the non-stationarity of neural oscillations, where amplitude and frequency change and the phase occasionally resets in unpredictable ways. In other words, if the oscillation were perfectly stationary, a 10 Hz peak at 70 ms would be perfectly predicted by a peak occurring at -30 and at 170 ms. However, since EEG signals are only weakly stationary, phase at these other time points only weakly predict phase at 70 ms. So, the success of previous literature at predicting stimulus observation using prestimulus time points could be attributed to the fact that these prestimulus time points will weakly predict phase at *t2*, but it is actually the phase at *t2* that best predicts observational outcome. This also explains the weakened effects found when measuring phase and amplitude at *t0* in the present study.

ATTENTION

Given the alpha rhythm's known negative correlation with attention, the results of this study are consistent with theories that the alpha rhythm facilitates attention by effectively down-sampling incoming sensory information that has been deemed irrelevant to conserve resources for more important neural processes. Speculatively, down-sampling irrelevant sensory information could be beneficial by reducing cortical processing load and metabolic consumption, as suggested by Callaway and Alexander (1960) who referred to this supposed sampling as a "neuronic shutter". And, as suggested in the "pulsed inhibition" account of alpha oscillations by Mathewson et al. (2009), rather than totally blocking out irrelevant information, sampling the sensory stream would be more prudent in case something relevant does occur and needs to be attended to.

It has been shown using simultaneous EEG, fMRI, and PET imaging techniques that increased alpha power over a sensory cortex is correlated with reduced metabolic consumption in that cortex (Moosmann et al., 2003). Moosmann et al. (2003) speculated that this reduced energy consumption could be due simply to the reduced informational input (as a result of sampling) or to the increased cellular efficiency of synchronized membrane oscillations in processing and synaptic transmission. This point of cellular efficiency is complemented by Klimesch et al. (2007) who suggested that, in contrast to the "cortical-idling" hypothesis, alpha oscillations represent an active top-down inhibition process that defines strict time-windows during which processing can occur. In his "inhibition-timing" hypothesis, he proposes that this strict timing of informational transfer not only allows very for selective information processing, but also increases the efficiency of the informational transfer.

These above mentioned hypotheses of the alpha rhythm function, the "neuronic shutter", the "pulsed inhibition", and the "inhibition-timing" hypothesis all appear to be complementary, although perhaps stressing different aspects. The visual sampling effect found here is presented as support of each of these hypotheses and puts a finer point on the timing of the effect in a way that is suggestive of the underlying neural mechanism as will be discussed in the next section.

The prominence of the posterior alpha rhythm when eyes are closed may be due to an automatic implicit assumption that no relevant information could come in during this state,

and this automatic assumption may be difficult to override even when a task demands it such as did the one performed in the present study. Presumably, the findings of the present study would also extend to eyes open conditions, however, the prominence of the alpha rhythm in closed eye conditions made presenting images during times of high amplitude spontaneous oscillations most efficient. Future studies should conduct a similar analysis in both eyes open and closed conditions to see if the same effect persists.

NEURAL MECHANISM

Understanding the biological mechanism underlying alpha oscillation is important for explaining its function. Although simultaneous recordings with fMRI and PET correlated alpha activity with fluctuations in the thalamus, thus suggesting this might be the origin of alpha rhythm (Hughes et al., 2004; Omata et al., 2013), so far the precise mechanism in humans is not yet agreed on. However, sleep spindles, a ~10 Hz alpha-like oscillation that occurs in 1-3 second bursts during transition to sleep, do have a well-established mechanism. The sleep spindle mechanism includes a negative feedback loop between the LGN and the reticular nucleus (RN, shown in Figure 10). Both nuclei have T-type Ca+ channels that, when activated, exhibit burst firing. Between each burst of the LGN, the Ca+ channels of the LGN are known to enter a refractory period, and the RN sends a similar, but inhibitory, burst to the LGN. During this time, sensory information from the optic nerve would be less likely to be relayed to V1. Importantly, the refractory periods of these T-type Ca+ channels are known to result in each nucleus firing at a ~10 Hz rate (Lopes da Silva, 1991; Sherman, 2001; Timofeev and Bazhenov, 2005; Alexander et al., 2006; Timofeev

and Chauvette, 2011). Each LGN burst firing generates massive EPSPs in V1, measured as a negativity in the occipital EEG (Timofeev and Bazhenov, 2005) and producing the ~10 Hz oscillation of sleep spindles seen on EEG. Chen et al. (2016) showed that in mice, very similar mechanisms give rise to both sleep spindles and waking alpha oscillations, and that the mechanism is capable of phasically modulating sensory transfer through the thalamus, and on this basis, they predicted the perceptual results found here. In cats too, this mechanism was found to produce waking alpha oscillations with the same phasic sensory gating effect (Lorincz et al., 2009).

Although the sleep spindle mechanism has been found to be almost entirely thalamo-cortical, cortico-cortical mechanisms are also found to contribute to the alpha rhythm (Steriade et al., 1990). These cortico-cortical mechanisms appear to include local pacemakers in supragranular layers that drive the rhythm in other layers (Bollimunta et al., 2008), however Bollimunta et al. (2011) found that these cortico-cortical mechanisms dominate mainly in extrastriate regions, whereas the alpha rhythm of the primary visual cortex appears mainly to be driven by thalamo-cortical connections. There is much evidence supporting this thalamic mechanism as the primary driver of the posterior alpha rhythm (Hughes and Crunelli, 2005) and it is assumed here to be responsible for the observed phase effect on visual perception.

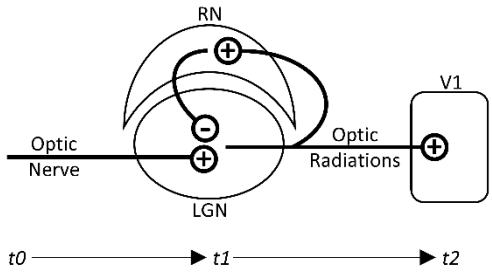

Figure 10. Visual pathway from retinal to V1.The LGN/RN negative feedback loop provides a mechanism of cycling LGN excitability state. This LGN/RN network is known to give rise to sleep spindles. The same, or a similar, mechanism is expected to give rise the posterior alpha rhythm.

CELLULAR SHUTTER EFFECT GENERATES A BEHAVIORAL GRADED GATING EFFECT

If the neural mechanism posited above were correct, the neuronic shutter effect would best be described as occurring at the level of individual LGN relay cells, in which the effect may occur at a nearly binary level. However, the behavioral effects we observe are graded, with increasing and decreasing probabilities of stimulus observation. This may be explained given that oscillating excitatory states are not always synchronized across all LGN cells. It is not necessarily the case that all cells are simultaneously in burst-mode firing state; some may concurrently operate in the normal tonic firing state. Thus, one cell may be in a state of inhibition and not relay to V1, while others may relay visual information as usual. However, in asynchronous states, the alpha rhythm should be decreased in amplitude. As shown in this study, at higher alpha amplitudes, the differences in observation rates between peak and trough phases at *t2* increased, presumably indicating that the measured phase becomes more representative of the excitatory state of larger

populations of LGN cells with increasing alpha amplitude. Asynchrony is also important to consider, not just among cells within an LGN, but between the LGNs of the left and right hemispheres. As on a cellular level, one LGN may restrict the flow of visual information while the other relays it. Presumably, if all cells within and between LGNs were in perfect synchrony, behavior relative to peak/trough phase at *t2* would reflect a perfect on/off visual shutter. This simple relationship wasn't observed in this study, and it is therefore more appropriate to describe the proposed neuronic shutter effect at the cellular level generating a graded, gating effect of perception at the behavioral level.

In sum, to our knowledge, this is the first study to examine the neuronic shutter effect with an exact phase and timing relationship to perceptual performance predicted by the underlying physiology of the visual system. The study design is novel and rigorous in controlling for individual visual conduction delays and hemispheric asynchrony. During times of high amplitude alpha oscillations, we found participants on average are most likely to perceive stimuli at waveform trough (272.41°) with observation rates 20.96% greater than at the opposing peak phase (92.41°). Given the rigor in our phase measurements, these results provide strong support for a mechanism that modulates perception described by the neuronic shutter effect and is reflected in the posterior alpha rhythm. Further studies with conduction delay-adjusted phase measurement are needed to investigate this shutter effect in the mu and tau rhythms over the sensorimotor and auditory cortices, to explore the possibility of this mechanism in other sensory systems.

Reductions in the alpha rhythm amplitude have been observed in, and used as a biomarker for, various pathological conditions, such as seizure disorders (Aich, 2014) and Alzheimer's disease (Prinz and Vitiello, 1989; Montez et al., 2009; Blinowska et al., 2017; Sharma and Nadkarni, 2020). Our novel technique of accounting for each individual's conduction delay could assist future investigations into more accurately identifying and measuring alpha rhythm changes observed in these pathological disorders. Given the variable severity of these disorders in patients, the ability to account for the biological differences among individuals is essential for successful early detection and diagnosis of these disorders using alpha rhythm changes.

REFERENCES

Aich TK (2014) Absent posterior alpha rhythm: An indirect indicator of seizure disorder? Indian J Psychiatry 56:61-66.

Alexander GM, Carden WB, Mu J, Kurukulasuriya NC, McCool BA, Nordskog BK, Friedman DP, Daunais JB, Grant KA, Godwin DW (2006) The Native T-Type Calcium Current in Relay Neurons of The. Neuroscience 141:453-461.

American Electroencephalographic Society (1994) Guideline thirteen: guidelines for standard electrode position nomenclature. American Electroencephalographic Society. J Clin Neurophysiol 11:111-113.

Ancoli S, Green KF (1977) Authoritarianism, Introspection, and Alpha Wave Biofeedback Training. Psychophysiology 14:40-44.

Babiloni C, Del Percio C, Arendt-Nielsen L, Soricelli A, Romani GL, Rossini PM, Capotosto P (2014) Review: Cortical EEG alpha rhythms reflect task-specific somatosensory and motor interactions in humans. In: Clinical Neurophysiology, pp 1936-1945: Elsevier Ireland Ltd.

Barry RJ, Clarke AR, Johnstone SJ, Magee CA, Rushby JA (2007) EEG differences between eyes-closed and eyes-open resting conditions. Clinical Neurophysiology 118:2765-2773.

Bastiaansen MC, Brunia CH (2001) Anticipatory attention: an event-related desynchronization approach. Int J Psychophysiol 43:91-107.

Bazanova OM, Aftanas LI (2008) Individual measures of electroencephalogram alpha activity and non-verbal creativity. Neurosci Behav Physiol 38:227-235.

Bazanova OM, Vernon D (2014) Review: Interpreting EEG alpha activity. Neuroscience and Biobehavioral Reviews 44:94-110.

Ben-Simon E, Podlipsky I, Okon-Singer H, Gruberger M, Cvetkovic D, Intrator N, Hendler T (2013) The Dark Side of the Alpha Rhythm: fMRI Evidence for Induced Alpha Modulation During Complete Darkness. European Journal of Neuroscience 37:795-803.

Berens P (2009) CircStat: A MATLAB Toolbox for Circular Statistics. Journal of Statistical Software 31:21.

Bierings RAJM, Kuiper M, Van Berkel CM, Overkempe T, Jansonius NM (2018) Foveal Light and Dark Adaptation in Patients With Glaucoma and Healthy Subjects: A Case-Control Study. PLoS ONE 13.

Bland JM, Altman DG (1995) Multiple Significance Tests: The Bonferroni Method. BMJ: British Medical Journal 310:170-170.

Blinowska KJ, Rakowski F, Kaminski M, De Vico Fallani F, Del Percio C, Lizio R, Babiloni C (2017) Functional and effective brain connectivity for discrimination between Alzheimer's patients and healthy individuals: A study on resting state EEG rhythms. Clin Neurophysiol 128:667-680.

Bollimunta A, Chen Y, Schroeder CE, Ding M (2008) Neuronal mechanisms of cortical alpha oscillations in awake-behaving macaques. J Neurosci 28:9976-9988.

Bollimunta A, Mo J, Schroeder CE, Ding M (2011) Neuronal mechanisms and attentional modulation of corticothalamic alpha oscillations. J Neurosci 31:4935-4943.

Brainard DH (1997) The Psychophysics Toolbox. Spatial Vision 10:433-436.

Bruers S, VanRullen R (2018) Alpha Power Modulates Perception Independently of Endogenous Factors. Frontiers in Neuroscience 12:279.

Callaway E, Alexander JD (1960) The Temporal Coding of Sensory Data: An Investigation of Two Theories. Journal of General Psychology 62:293-309.

Chen Z, Wimmer RD, Wilson MA, Halassa MM (2016) Thalamic Circuit Mechanisms Link Sensory Processing in Sleep and Attention. In, pp 83-83.

Clark VP, Fan S, Hillyard SA (1995) Identification of Early Visual Evoked Potential Generators by Retinotopic and Topographic Analyses. Human Brain Mapping 2:170-187.

Cohen MX (2014) Analyzing Neural Time Series Data: Theory and Practice: MIT Press.

Cohen MX (2019) A Better Way to Define and Describe Morlet Wavelets for Time-Frequency Analysis. NeuroImage 199:81-86.

Compston A (2010) The Berger rhythm: potential changes from the occipital lobes in man. Brain 133:3-6.

Cooper NR, Croft RJ, Dominey SJJ, Burgess AP, Gruzelier JH (2003) Paradox Lost? Exploring the Role of Alpha Oscillations During Externally vs Internally Directed Attention and the Implications for Idling and Inhibition Hypotheses. International Journal of Psychophysiology 47:65-74.

Cornsweet TN (1962) The Staircase Method in Psychophysics. The American Journal of Psychology 75:485-491.

Delorme A, Makeig S (2004) EEGLAB: an Open Source Toolbox for Analysis of Single-Trial EEG Dynamics Including Independent Component Analysis. Journal of Neuroscience Methods 134:9-21.

Di Russo F, Martínez A, Sereno MI, Pitzalis S, Hillyard SA (2001) Cortical Sources of the Early Components of the Visual Evoked Potential. Human Brain Mapping 15:95-111.

Dustman RE, Beck EC (1965) Phase of Alpha Brain Waves, Reaction Time and Visually Evoked Potentials. Electroencephalogr Clin Neurophysiol 18:433-440.

Ergenoglu T, Demiralp T, Bayraktaroglu Z, Ergen M, Beydagi H, Uresin Y (2004) Alpha rhythm of the EEG modulates visual detection performance in humans. Cognitive Brain Research 20:376-383.

Garcia-Rill E, D'Onofrio S, Luster B, Mahaffey S, Urbano FJ, Phillips C (2016) The 10 Hz Frequency: A Fulcrum For Transitional Brain States. Transl Brain Rhythm 1:7-13.

Gonçalves SI, de Munck JC, Pouwels PJW, Schoonhoven R, Kuijer JPA, Maurits NM, Hoogduin JM, Van Someren EJW, Heethaar RM, Lopes da Silva FH (2006) Correlating the alpha rhythm to BOLD using simultaneous EEG/fMRI: Inter-subject variability. Neuroimage 30:203-213.

Hartmann T, Schlee W, Weisz N (2012) It's only in your head: expectancy of aversive auditory stimulation modulates stimulus-induced auditory cortical alpha desynchronization. Neuroimage 60:170-178.

Hughes SW, Crunelli V (2005) Thalamic mechanisms of EEG alpha rhythms and their pathological implications. In, pp 357-372.

Hughes SW, Lorincz M, Cope DW, Blethyn KL, Kekesi KA, Parri HR, Juhasz G, Crunelli V (2004) Synchronized Oscillations at Alpha and Theta Frequencies in the Lateral Geniculate Nucleus. In, pp 253-268: Neuron.

Janssens C, De Loof E, Nico Boehler C, Pourtois G, Verguts T (2018) Occipital Alpha Power Reveals Fast Attentional Inhibition of Incongruent Distractors. Psychophysiology 55:1-11.

Kizuk SA, Mathewson KE (2017) Power and Phase of Alpha Oscillations Reveal an Interaction between Spatial and Temporal Visual Attention. J Cogn Neurosci 29:480-494.

Kleiner M, Brainard D, Pelli D, Ingling A, Murray R, Broussard C (2007) What's New in Psychtoolbox-3. In, pp 1-16.

Klimesch W, Sauseng P, Hanslmayr S (2007) EEG alpha oscillations: the inhibition-timing hypothesis. Brain Res Rev 53:63-88.

Klimesch W, Fellinger R, Freunberger R (2011) Alpha oscillations and early stages of visual encoding. Front Psychol 2:118.

Knyazev GG, Levin EA, Savostyanov AN (2008) Impulsivity, anxiety, and individual differences in evoked and induced brain oscillations. Int J Psychophysiol 68:242-254.

Legewie H, Simonova O, Creutzfeldt OD (1969) EEG changes during performance of various tasks under open- and closed-eyed conditions. Electroencephalography & Clinical Neurophysiology 27:470-479.

Limbach K, Corballis PM (2017) Alpha-power modulation reflects the balancing of task requirements in a selective attention task. Psychophysiology 54:224-234.

Lindsley DB (1952) Psychological phenomena and the electroencephalogram. Electroencephalography & Clinical Neurophysiology 4:443-456.

Lopes da Silva F (1991) Neural Mechanisms Underlying Brain Waves: From Neural Membranes. Electroencephalography and Clinical Neurophysiology 79:81-93.

Lopez-Calderon J, Luck SJ (2014) ERPLAB: An Open-Source Toolbox for the Analysis of Event-Related Potentials. Frontiers in Human Neuroscience 8.

Lorincz ML, Kekesi KA, Juhasz G, Crunelli V, Hughes SW (2009) Temporal framing of thalamic relay-mode firing by phasic inhibition during the alpha rhythm. Neuron 63:683-696.

Mathewson KE, Gratton G, Fabiani M, Beck DM, Ro T (2009) To See or Not to See: Prestimulus Alpha Phase Predicts Visual Awareness. Journal Of Neuroscience 29:2725-2732.

Mathewson KE, Prudhomme C, Fabiani M, Beck DM, Lleras A, Gratton G (2012) Making Waves in the Stream of Consciousness: Entraining Oscillations in EEG Alpha and Fluctuations in Visual Awareness With Rhythmic Visual Stimulation. Journal Of Cognitive Neuroscience 24:2321-2333.

Milton A, Pleydell-Pearce CW (2016) The phase of pre-stimulus alpha oscillations influences the visual perception of stimulus timing. Neuroimage 133:53-61.

Montez T, Poil SS, Jones BF, Manshanden I, Verbunt JP, van Dijk BW, Brussaard AB, van Ooyen A, Stam CJ, Scheltens P, Linkenkaer-Hansen K (2009) Altered temporal correlations in parietal alpha and prefrontal theta oscillations in early-stage Alzheimer disease. Proc Natl Acad Sci U S A 106:1614-1619.

Moosmann M, Ritter P, Krastel I, Brink A, Thees S, Blankenburg F, Taskin B, Obrig H, Villringer A (2003) Correlates of alpha rhythm in functional magnetic resonance imaging and near infrared spectroscopy. Neuroimage 20:145-158.

Omata K, Hanakawa T, Morimoto M, Honda M (2013) Spontaneous Slow Fluctuation of EEG Alpha Rhythm Reflects Activity in Deep-Brain Structures: A Simultaneous EEG-fMRI Study. PLoS ONE 8:1-12.

Pavlenko VB, Chernyi SV, Goubkina DG (2009) EEG Correlates of Anxiety and Emotional Stability in Adult Healthy Subjects. In: Neurophysiology, pp 337-345.

Pelli DG (1997) The VideoToolbox software for visual psychophysics: Transforming numbers into movies. Spatial Vision 10:437-442.

Pfurtscheller G, Stancák A, Jr., Neuper C (1996) Event-related synchronization (ERS) in the alpha band--an electrophysiological correlate of cortical idling: a review. International journal of psychophysiology : official journal of the International Organization of Psychophysiology 24:39-46.

Pineda JA (2005) The Functional Significance of Mu Rhythms: Translating “Seeing” and “Hearing” Into “Doing”. Brain Research Reviews 50:57-68.

Prinz PN, Vitiello MV (1989) Dominant occipital (alpha) rhythm frequency in early stage Alzheimer's disease and depression. Electroencephalogr Clin Neurophysiol 73:427-432.

Ray WJ, Cole HW (1985) EEG Alpha Activity Reflects Attentional Demands, and Beta Activity Reflects Emotional and Cognitive Processes. Science 228:750-752.

Sauseng P, Klimesch W, Stadler W, Schabus M, Doppelmayr M, Hanslmayr S, Gruber WR, Birbaumer N (2005) A Shift of Visual Spatial Attention is Selectively Associated With Human EEG Alpha Activity. The European Journal Of Neuroscience 22:2917-2926.

Seeck M, Koessler L, Bast T, Leijten F, Michel C, Baumgartner C, He B, Beniczky S (2017) The standardized EEG electrode array of the IFCN. Clin Neurophysiol 128:2070-2077.

Sharma R, Nadkarni S (2020) Biophysical basis of alpha rhythm disruption in Alzheimer's Disease (AD). eNeuro.

Sherman SM (2001) Tonic and Burst Firing: Dual Modes of Thalamocortical Relay. TRENDS in Neurosciences 24:122-126.

Steriade M, Gloor P, Llinas RR, Lopes de Silva FH, Mesulam MM (1990) Basic mechanisms of cerebral rhythmic activities. Electroencephalogr Clin Neurophysiol 76:481-508.

Tenke CE, Kayser J, Alvarenga JE, Abraham KS, Warner V, Talati A, Weissman MM, Bruder GE (2018) Temporal stability of posterior EEG alpha over twelve years. Clin Neurophysiol 129:1410-1417.

Tenke CE, Kayser J, Svob C, Miller L, Alvarenga JE, Abraham K, Warner V, Wickramaratne P, Weissman MM, Bruder GE (2017) Association of Posterior EEG Alpha With Prioritization of Religion or Spirituality: A Replication and Extension at 20-Year Follow-Up. Biological Psychology 124:79-86.

Tiihonen J, Hari R, Kajola M, Karhu J, Ahlfors S, Tissari S (1991) Magnetoencephalographic 10-Hz Rhythm From the Human Auditory Cortex. Neuroscience Letters 129:303-305.

Timofeev I, Bazhenov M (2005) Mechanisms and Biological Role of Thalamocortical Oscillations.

Timofeev I, Chauvette S (2011) Thalamocortical Oscillations: Local Control of EEG Slow Waves. Current Topics in Medicinal Chemistry 11:2457-2471.

VanRullen R, Koch C (2003) Is perception discrete or continuous? Trends in Cognitive Sciences 7:207-213.

VanRullen R, Zoefel B, Ilhan B (2014) On the cyclic nature of perception in vision versus audition. Philos Trans R Soc Lond B Biol Sci 369:20130214.

Weisz N, Hartmann T, Müller N, Lorenz I, Obleser J (2011) Alpha Rhythms in Audition: Cognitive and Clinical Perspectives. Frontiers in Psychology 2:1-15.

Wieneke GH, Deinema CH, Spoelstra P, Storm van Leeuwen W, Versteeg H (1980) Normative spectral data on alpha rhythm in male adults. Electroencephalography and clinical neurophysiology 49:636-645.

Yue W, Chun NW, Siong NK, Tiecheng W, Xiaoping L (2013) An EEG Source Localization and Connectivity Study on Deception of Autobiography Memories. In, pp 468-471: IEEE.